CivilEng

MDPI

Article

Study of Dynamic Modulus of Asphalt Mix after Reinforcement of Sandstone

Bowen Zhang [1], Shuangquan Jiang [1,2], Nanxiang Zheng [1,*], Jinduo Liu [1,3] and Yuxing Wang [1]

[1] College of Highway, Chang'an University, Xi'an 710064, China; 13195476671@163.com (B.Z.); jiangsq5311@126.com (S.J.); ljd2568206385@163.com (J.L.); 15668358592@163.com (Y.W.)
[2] Sichuan Highway and Bridge Construction Group Limited, Chengdu 610041, China
[3] Jiaoke Transport Consultans Ltd., Beijing 100083, China
* Correspondence: emailznx@163.com

Abstract: Sandstone has poor mechanical properties. To facilitate the application of sandstone into asphalt mixtures, sandstone was treated by immersion in sodium silicate solution, and the dynamic modulus after reinforcement was used as a criterion. The results showed that the mechanical properties of the sandstone aggregate treated with sodium silicate were improved, and the dynamic modulus was increased by 18.2%, which will help to reduce rutting. The dynamic modulus and phase angle can be effectively predicted over a wide frequency range using the sigma function and the Kramers–Kronig relationship. Sandstone asphalt mixtures basically conform to linear viscoelasticity, but the phase angle changes are more complicated at high temperatures and do not vary monotonically with frequency. By calculating the rutting coefficient, fatigue coefficient, and DSRFn parameters for performance prediction, it was found that an increase in dynamic modulus resulted in a significant increase in the rutting coefficient but a decrease in the cracking resistance.

Keywords: asphalt mixtures; sodium silicate solution; reinforcement; sandstone; dynamic modulus

check for updates

Citation: Zhang, B.; Jiang, S.; Zheng, N.; Liu, J.; Wang, Y. Study of Dynamic Modulus of Asphalt Mix after Reinforcement of Sandstone. *CivilEng* **2024**, *5*, 852–865. https://doi.org/10.3390/civileng5040044

Academic Editors: Angelo Luongo and Luis Picado-Santos

Received: 24 July 2024
Revised: 4 September 2024
Accepted: 9 September 2024
Published: 30 September 2024

Copyright: © 2024 by the authors. Licensee MDPI, Basel, Switzerland. This article is an open access article distributed under the terms and conditions of the Creative Commons Attribution (CC BY) license (https://creativecommons.org/licenses/by/4.0/).

1. Introduction

As the mileage of highways continues to increase, the demand for traditional high-quality materials such as limestone and basalt, which are essential for construction, will also rise. This will inevitably lead to a shortage of stone materials. Sandstone is not a traditional stone with excellent performance, but it is widely distributed in Sichuan, so if it can be used in road construction, it can effectively reduce the consumption of traditional stone and the cost of transport to other places.

In recent years, there have been instances where sandstone has been employed in road construction. Fan, Jianwei [1], and others demonstrated the feasibility of siliceous sandstone as a porous asphalt mixture by comparing the road performance of siliceous sandstone and limestone mixtures. However, using a sandstone mixture in frosty areas in winter is not recommended. Li, Haibin et al. [2] compare the effects of practically applying sandstone and limestone, placing a particular focus on grass-roots level application. However, it should be noted that sandstone has a superior water absorption ability and greater porosity than limestone, which may impact the mechanical properties of sandstone. Bao Xingwei et al. [3] investigated the use of sandstone in the middle surface layer, ensuring that the mixture met the basic requirements for high-temperature performance and water stability. Ma, Xiaohui et al. [4] investigated the use of sandstone in the upper layer and enhanced its adhesion with a specific quantity of cement; they suggested that anti-spalling agents should be incorporated. Bingyang Li [5] evaluated the impact of water content on the mechanical properties of rock and discovered that powdered sandstone exhibits diminished compressive strength and elastic modulus with increasing water content. Although sandstone can be used as a pavement material, its inherent problems, such as low compressive strength and high-water absorption, remain unresolved. There have

been fewer studies on the dynamic modulus of sandstone mixes, which is important for pavement design and performance evaluation.

Chen Wenwu [6] and other researchers have demonstrated that the mechanical strength and salt durability of sandstone can be enhanced through artificial aging of the stone followed by immersing it in a high-molar ratio potassium silicate solution. Yumeng et al. [7] observed a significant increase in the strength of recycled aggregates and a reduction in voids when incorporating soaking in sodium silicate solution into their process. Tang Shiliang and colleagues [8] showed that mixing sandstone with a sodium silicate solution can effectively reduce its porosity, thereby enhancing its mechanical properties. Sodium silicate solution is widely used in the road industry due to its inexpensive nature and significant strengthening effect. To make the sandstone aggregate have good mechanical properties and water absorption, sodium silicate solution is used for the immersion strengthening treatment of the sandstone aggregate, and then the dynamic modulus before and after the treatment and the change rule of the phase angle are studied, establishing the dynamic modulus, phase angle, and other master curves to study the linear viscoelasticity of the mixture, and finally calculating the rutting factor, fatigue factor, and DSRFn parameter to predict the performance changes of the mixture.

2. Material Technical Index

2.1. Reinforcement Materials

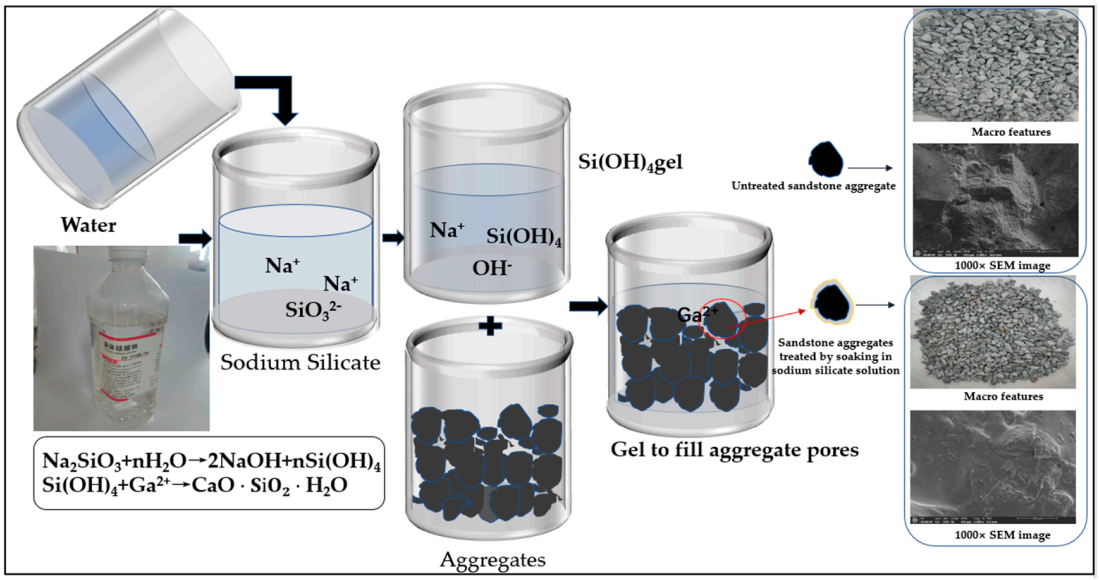
The reinforcing agent that we used in this study is a sodium silicate solution produced by China Jiashan Yurui Refractories Co. Sodium (Jiaxing, China) silicate was dissolved in the solution to produce an aqueous silica gel solution, which was then applied to the surface of the aggregate to fill any defects. The preparation process entailed the addition of a sodium silicate stock solution to water, resulting in the formation of a 20% sodium silicate solution (it should be noted that the reduction in the water absorption of the aggregate decreases significantly when the concentration exceeds 20%). Following this, the reinforced aggregate was subjected to a one-day soaking period. The specific reinforcement mechanism and the comparison using SEM and exterior images are shown in Figure 1 below. Table 1 provides a detailed overview of the technical parameters of the product.

Table 1. Indicators of the sodium silicate solution's properties.

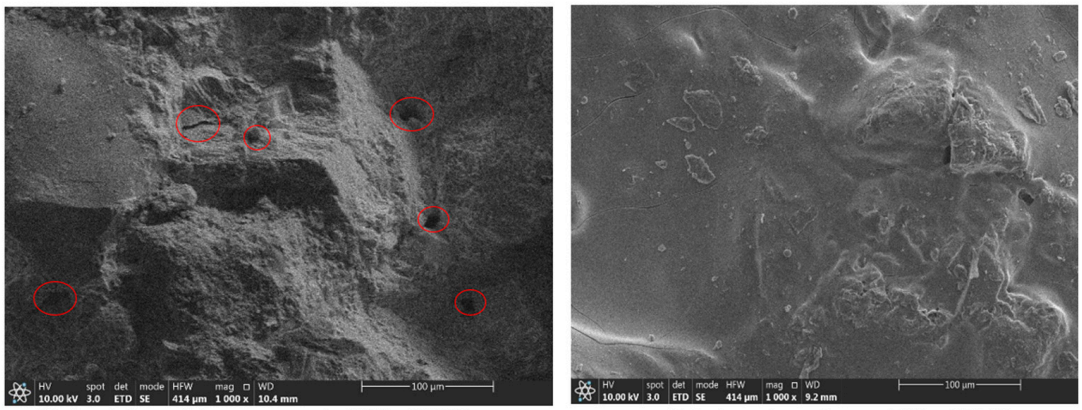
Technical Indicators	Results
Densities (20 °C)/g/mL	1.385
Silicon dioxide mass fraction/%	26.98
Mass fraction of oxidized Na/%	8.53
Baume degrees (20 °C)/°Bé	38.5
Modulus/(M)	3.30

Please refer to Figure 1 for further details. There was no significant change in the macroscopic appearance of the surface, but from the 1000× SEM image it can be observed that there were more voids and tiny cracks on the surface of the untreated aggregate (which is also the reason for the high-water absorption of the original aggregate), whereas, in the case of the sodium silicate solution-treated aggregate, the pores were significantly reduced in the presence of gel-encapsulated aggregates on the surface.

Sodium silicate dissolved in water will first undergo a hydrolysis reaction, generating NaOH and water-containing silica gel $[Si(OH)_4]n$. $Si(OH)_4$ can react with free Ca^{2+} on the surface of sandstone aggregate to generate hydrated calcium silicate (C-S-H) gel, and the new hydration product fills and articulates in the network structure, making the aggregate surface structure dense.



(**a**)



(**b**)

Figure 1. The strengthening mechanism and macro-micro comparison. (**a**) Sodium silicate treatment process; (**b**) SEM image of sandstone aggregate before and after treatment.

2.2. Comparison of Strengthening Results

The relevant methods outlined in the "Aggregate Experiment Specification for Highway Engineering" (JTGE42-2005) [9] should be employed to conduct experiments aimed at obtaining the requisite technical indexes; we conducted such experiments, and the results are detailed in Table 2.

The experimental results presented in Table 2 demonstrate that the original aggregate exhibits a higher apparent relative density, water absorption, crushing value, abrasion value, and robustness. However, these values do not meet the specified criteria. Treatment with sodium silicate solution was employed to enhance these parameters, resulting in a reduction in the values of certain properties. Nevertheless, the aggregate has shown improved performance and meets the required standards for the relevant properties.

Table 2. Comparison of aggregates before and after sodium silicate solution immersion treatment.

Technical Indicator		Unprocessed Aggregates	Reinforced Aggregates	Standardized Requirements
Apparent relative density/(g/cm^3)	15–20 mm	2.628	2.543	≥2.5
	10–15 mm	2.610	2.586	≥2.5
	5–10 mm	2.609	2.609	≥2.5
Water absorption/%	15–20 mm	2.663	2.475	≤3.0
	10–15 mm	3.031	2.740	≤3.0
	5–10 mm	3.811	3.722	≤3.0
Crushing value/%		28.9	19.8	≤28
wear value/%		33.8	26.4	≤30
ruggedness/%		19.1	8.2	≤12

2.3. Asphalt

Sandstone with a high SiO_2 content and acidic lithology usually has poor adhesion with asphalt. It is recommended to use SBS (Styrene-Butadiene-Styrene Block Copolymer) modified asphalt and to check the asphalt indexes according to the following Table 3. Our experiments were conducted according to the Specifications for Design and Construction of Asphalt Pavement of Expressway, specifically those pertaining to Sichuan Province, China.

Table 3. The results and measurements recorded for the modified asphalt.

Technical Indicator		Result	Standardized Requirements
Penetration of a needle/(25 °C, 100 g, 5 s)/0.1 mm		55	≥50
Softening point/°C		80	≥75
Ductility/(5 °C, 5 cm/min)/cm		32	≥20
Flash point/°C		260	≥230
Solubility/%		99.6	≥99
Solubility/%		99.6	≥99
Kinematic viscosity 135 °C/Pa·s		2.42	≤3
Elastic recovery 25 °C/%		96	≥90
Dynamic shear DSR76 °C (G* [1]/sinδ@10 rad/s)/KPa		1.84	≥1.0
Residues after RTFOT	Mass change/%	−0.03	≤±1.0
	Needle penetration ratio (25 °C)/%	72	≥65
	Elongation (5 °C, 5 cm/min)/cm	17	≥15
	Dynamic shear DSR76 °C (G*/sinδ@10 rad/s)/KPa	2.56	≥2.2

[1] G*: Dynamic shear modulus.

2.4. Other Materials

The crushing of sandstone results in the production of stone chips with a high content of particles smaller than 0.075 mm. To prevent an excess of fine aggregate, in this study, limestone was chosen as the fine aggregate.

3. Design of Mix Ratio

3.1. Grading Design

The grading curve should be adjusted in accordance with the sieving results of the aggregate. The AC-20 type dense grading design should be adopted the grading curve is illustrated in Figure 2 below.

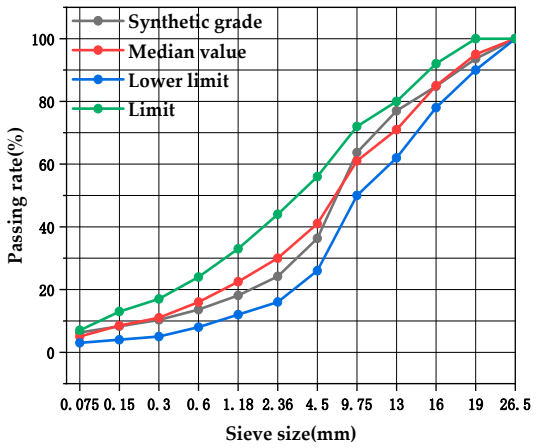


Figure 2. Grading curve.

3.2. Optimum Asphalt Content

The optimal asphalt content for the asphalt mixture was determined using the Marshall test. The optimal asphalt dosage for the untreated sandstone mixture was found to be 5.21%. For the reinforced sandstone mixture, the optimal asphalt dosage was determined to be 5.03%, and the effect of sodium silicate solution treatment on the asphalt dosage was found to be negligible.

4. Dynamic Modulus

Our experiments were based on the "Standard Test Methods of Bitumen and Bituminous Mixtures for Highway Engineering".

To simulate the compaction of the mix by a field roller, the test specimens were molded by rotary compaction. The untreated sandstone aggregates that we used are shown in Figure 3a, while the aggregates treated with sodium silicate solution are shown in Figure 3b. The reinforced sandstone aggregate was prepared by creating Ø150 × 170 mm specimens, which were then drilled to create Ø100 × 150 mm specimens. The test temperatures were set at −10 °C, 20 °C, and 50 °C, and a holding time of 4 h was adopted. The specimens were evaluated using the basic performance of the Asphalt Mixture Testing System (SPT). Finally, holes were drilled to produce Ø100 × 150 mm specimens. The asphalt mixture's basic performance was evaluated using a dynamic modulus tester system, enabling the observation of changes in dynamic modulus across different loading frequencies. The selected loading frequencies were 0.1 Hz, 0.5 Hz, 1 Hz, 10 Hz, and 25 Hz. The specimens and experimental apparatus are depicted in Figure 3 below.

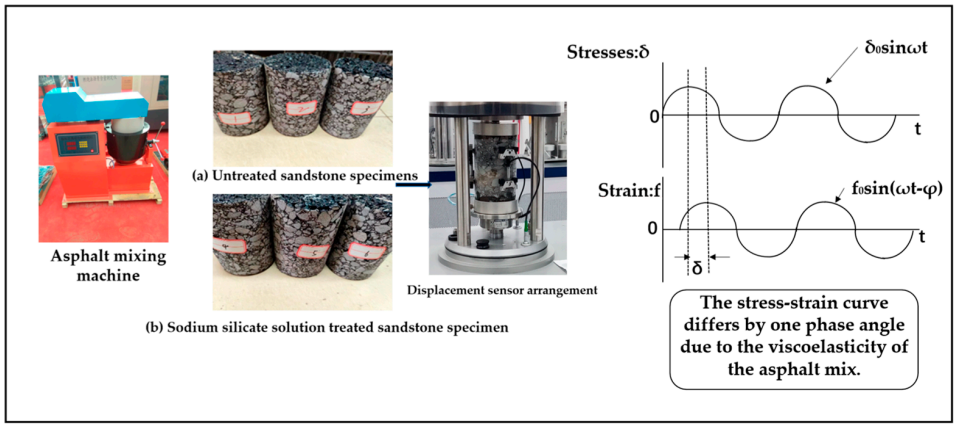


Figure 3. Specimen and test apparatus. (**a**) Untreated sandstone specimens; (**b**) Sodium silicate solution treated sandstone specimen.

5. Results and Discussions

5.1. Dynamic Modulus Test Results and Analysis

Dynamic modulus is defined as a measure of the stiffness of an asphalt mix and plays a key role in pavement design, structural analysis, and durability prediction. The test data were processed to plot the trends in dynamic modulus and phase angle of asphalt mixes with test temperature and loading frequency, as shown in Figure 4. The test results are shown in Table 4 below. The values labeled "Reinforced Sandstone 50 °C" refer to a mix containing reinforced sandstone as an aggregate at 50 °C. Other values are similarly presented.

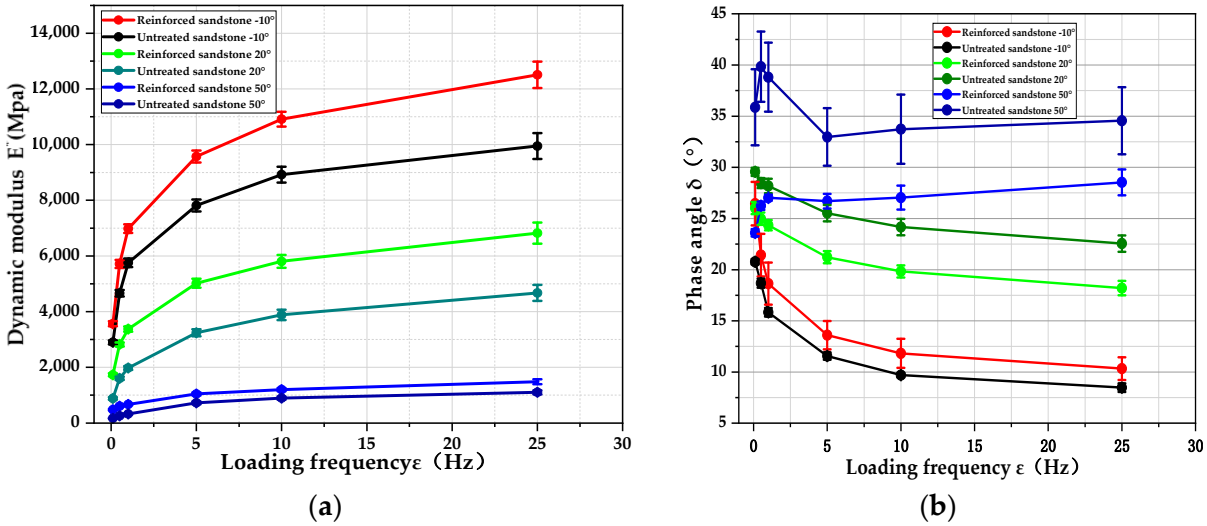


Figure 4. Dynamic modulus and phase angle test results. (**a**) Curve of the dynamic modulus of the mix with the loading frequency; (**b**) variation curve of the phase angle δ of the mix with the loading frequency.

Table 4. Dynamic modulus results.

Types	Loading Frequency (Hz)	Dynamic Modulus (MPa)			Phase Angle (°)		
		−10°	20°	50°	−10°	20°	50°
Reinforced sandstone	0.1	3567	1731	478	26.45	26.02	23.6
	0.5	5712	2823	607	21.42	24.98	26.24
	1	6983	3374	667	18.64	24.34	27.03
	5	9572	5021	1043	13.6	21.22	26.7
	10	10,912	5806	1199	11.83	19.83	27.04
	25	12,508	6821	1486	10.33	18.2	28.53
Untreated sandstone	0.1	2899	883.5	168	20.77	29.56	35.87
	0.5	4661	1603	254	18.68	28.46	39.84
	1	5756	1979	328	15.83	28.18	38.81
	5	7813	3241	725	11.56	25.52	32.97
	10	8920	3883	897	9.7	24.16	33.73
	25	9949	4674	1102	8.48	22.55	34.55

As illustrated in Figure 4, the trends in dynamic modulus and phase angle before and after reinforcement are essentially identical. This is because asphalt mixtures are viscoelastic materials exhibiting non-instantaneous deformation under load and showing hysteresis. Under low-frequency/high-temperature conditions, the mix exhibits lower dynamic modulus, a higher phase angle, and greater cohesion, which is why rutting is more severe in the summer or at long longitudinal slopes [10,11]. As the frequency increases (at low temperatures), the phase angle decreases, indicating that the elastic component is more pronounced

at high frequencies (low temperatures) and that the hysteresis phenomenon is reduced. However, it is worth noting that the phase angle tends to increase at 50 °C, as shown in Figure 4b. This trend has been observed in numerous experiments, and it has been postulated that the separation of measurement points may be attributed to elevated temperatures. To prevent this phenomenon, reducing the stress level is recommended [12,13].

The dynamic modulus of the reinforced sandstone was greater than that of the untreated sandstone at both 20 °C and 10 Hz, increasing by 45%. The phase angle exhibited a reversed trend, indicating that the phase lag will be reduced and the relative deformation will be more pronounced following the enhancement of the aggregate properties. This will result in an increase in the modulus. The reinforcement effect of sodium silicate aqueous solution-reinforced sandstone decreases with increasing temperature. This is because at high temperatures, the bitumen becomes softer and more fluid, leading to a smaller increase in modulus. The rate of decrease in phase angle before and after reinforcement was greater at high temperatures than at low temperatures. It is hypothesized that at low temperatures, bitumen plays a very important role, leading to some limitations in reducing the phase angle by reinforcing the aggregates.

5.2. Master Curve Analysis

5.2.1. Dynamic Modulus Master Curve

According to viscoelastic mechanics, the modulus of a material is the ratio of stress to strain. Since stress and strain are functions of time, the modulus of an asphalt mix will also vary with time and is known as the complex modulus. The complex modulus is usually expressed as shown in Equation (1):

$$E^* = E' + iE'' \tag{1}$$

where E′(ε) and E″(ε) are the real and imaginary parts of the complex modulus; ε = angular frequency, and $i^2 = -1$.

For viscoelastic materials at different temperatures and frequencies, they can be connected into a smooth curve to form a sigmoidal function. as shown in Equation (2) [14,15].

$$\lg|E^*(\varepsilon)| = \delta + \frac{\alpha}{1 + e^{\beta+\gamma\lg\varepsilon}} \tag{2}$$

In the above equation, E*(ε) is the dynamic modulus; ε is the loading frequency; δ is the minimum value of dynamic modulus/MPa; δ + α is the maximum value of dynamic modulus/MPa; α is variable; and β, γ are regression coefficients.

The temperature shift factor for viscoelastic materials can be calculated from the time-temperature equivalent equation and can be accurately predicted over a wide frequency range [16]. There are numerous expressions for α_T, of which the Williams-Landel-Ferry equation predicts the most accurate shift factor [17], as demonstrated in the WLF equation (Equation (3)).

$$\lg\alpha_T = \frac{-C1 \times (T - T_0)}{C2 + T - T_0} \tag{3}$$

In the above, C_1 and C_2 are the fitting parameters, T denotes the selected temperature, and T_0 denotes the reference temperature.

The reference temperature is set at 20 °C. The dynamic modulus master curves, illustrated in the following Figure 5, are characterized by converting the frequencies at different temperatures to the frequency at the reference temperature. The horizontal shift factor is employed to horizontally shift the data for the other temperatures to the 20 °C master curve. This adjustment makes several master curves fit more closely into a smooth line at the same shift distance. The values of the fitted parameters for the master curve are shown in Table 5 below.

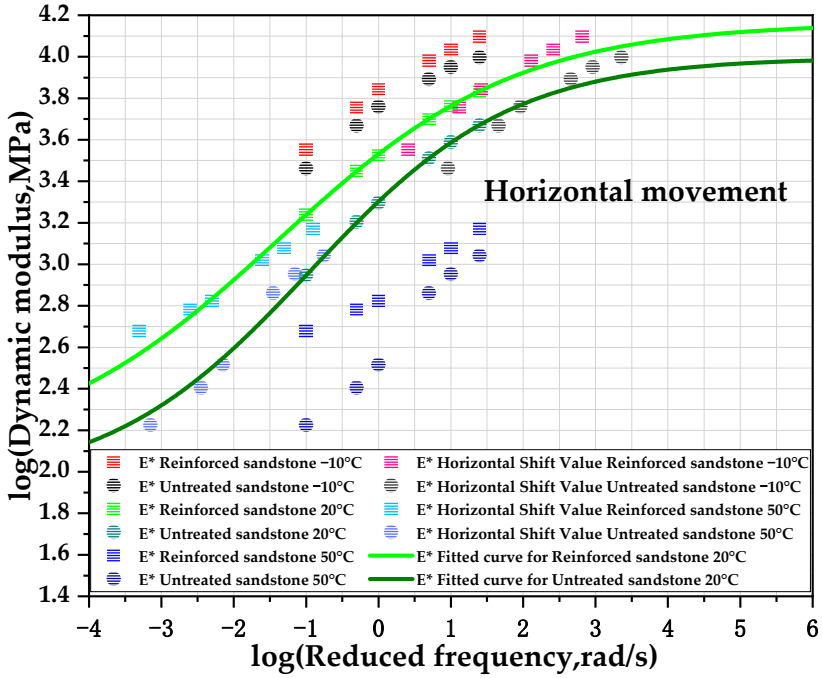


Figure 5. Dynamic modulus master curves at 20 °C.

Table 5. Parameters of dynamic modulus master curve.

Parameter	Reinforced Sandstone	Untreated Sandstone
δ	2.061	1.931
α	2.809	2.82
β	−0.575	−0.413
γ	−0.451	−0.496
R^2	0.999	0.999

As illustrated in Figure 5, the sigma formula exhibits remarkable consistency across a range of temperatures, with the kinetic modulus displaying a smooth, linear trajectory. The class 'S' curve, with an R^2 value of 0.99, provides strong evidence that the main curve of the kinetic modulus aligns with the theoretical framework of linear viscoelasticity. It can be observed that as the frequency increases, the growth rate of the dynamic modulus initially rises and then falls. The dynamic modulus of the reinforced sandstone is greater than that of the untreated material, indicating that the improvement in the dynamic modulus achieved through aggregate treatment is consistent with the desired outcome. The treatment of aggregates effectively enhances the modulus of asphalt mixtures. Although the theoretical maximum value of the dynamic modulus can be obtained due to the S-curve property, this was not confirmed in the actual experiment due to the many difficult-to-control factors affecting the dynamic modulus, such as the void ratio and mineral gap ratio.

5.2.2. Phase Angle Master Curve

Nevertheless, there are inherent limitations in the ability to describe the viscoelasticity of a material through the use of dynamic modulus versus reduced frequency curves. Additionally, changes in the viscoelastic portion cannot be observed intuitively [18]. Instead, E* (dynamic modulus), E′ (storage modulus), E″ (loss modulus), φ (phase angle), and ε are mathematically interrelated and share a common shift factor [17,19]. Furthermore, E* is related to E′ and E″ by the following equations (Equations (4) and (5)).

$$E' = |E^*| \times \cos\varphi \quad (4)$$

$$E'' = |E^*| \times \sin\varphi \tag{5}$$

The Kramers–Kronig equation effectively provides a way of using a mathematical method to establish a relationship between the real and imaginary parts of the complex modulus, which allows for the introduction of a relationship between the dynamic modulus and the phase angle in the presence of Equation (6) [20,21]. However, for asphalt mixtures, the phase angle does not exceed 45° at room temperature, so the phase angle needs to satisfy Equation (7) [18].

$$\varphi(\varepsilon) = \frac{\pi}{2}\frac{d(\lg|E^*|)}{d(\lg\varepsilon)} \tag{6}$$

$$0^\circ < \varphi < 45^\circ \tag{7}$$

Substituting the sigmoidal formula to fit the equation yields Equation (8) [21].

$$\varphi(\varepsilon) = -\frac{\pi}{2}\alpha\gamma\frac{e^{\beta+\gamma\lg\varepsilon}}{\left(1+e^{\beta+\gamma\lg\varepsilon}\right)^2} \tag{8}$$

Accordingly, the master curves of phase angle versus frequency before and after reinforcement are obtained as shown in Figure 6, where the parameter is in the parametric sigmoidal equation.

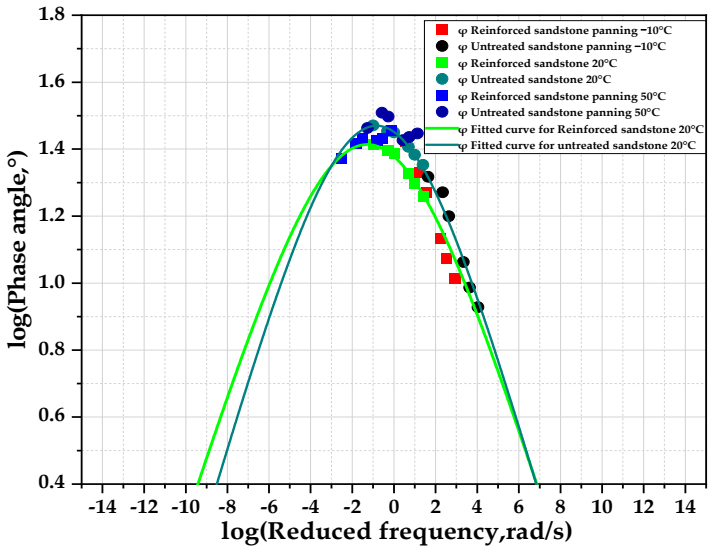


Figure 6. Phase angle master curve at 20 °C.

As illustrated in Figure 6, the primary curve of the phase angle exhibits a conventional bell shape. The phase angle aligns closely with this curve at medium and low temperatures, where the R^2 value for the reinforced sandstone is 0.99. The R^2 value for the untreated sandstone is 0.98. This indicates that the Kramers–Kronig (K–K) relationship effectively represents changes in the phase angle of the mixture. However, the trend of the phase angle becomes more complicated at high temperatures, as evidenced by the fact that the phase angle does not vary monotonically with increasing frequency, which is inconsistent with the linear viscoelastic behavior of the mixtures and may be related to the transition from viscoelastic to elastic behavior [22]. As the frequency increases, the phase angle rises to a peak and then decreases. This behavior is mainly observed at very low frequencies, where the mixture exhibits viscous properties. The increase in viscosity leads to greater delay, which corresponds to an increase in stress delay. When the frequency approaches approximately 0.08 rad/s, a peak is reached, followed by a decrease, possibly indicating a change in the material's behavior. Consequently, permanent deformation is more likely at high temperatures and low frequencies. The frequency at which the highest phase angle

value for the reinforced sandstone occurs and the overall trend are lower than those for untreated sandstone. This suggests that the elastic component and hysteresis delay of the reinforced sandstone are greater and lower, respectively, compared to untreated sandstone.

5.2.3. Storage Module Master Curve and Loss Module Master Curve

Based on Equations (4) and (5), along with the phase angle master curve and the dynamic modulus master curve, Equations (9) and (10) can be obtained.

$$E'(\varepsilon) = 10^{\delta+\alpha(1+e^{\beta+\gamma\lg\varepsilon})} \times \cos(10^{-\frac{\pi}{2}\alpha\gamma\frac{e^{\beta+\gamma\lg\varepsilon}}{(1+e^{\beta+\gamma\lg\varepsilon})^2}}) \quad (9)$$

$$E''(\varepsilon) = 10^{\delta+\alpha(1+e^{\beta+\gamma\lg\varepsilon})} \times \sin(10^{-\frac{\pi}{2}\alpha\gamma\frac{e^{\beta+\gamma\lg\varepsilon}}{(1+e^{\beta+\gamma\lg\varepsilon})^2}}) \quad (10)$$

The storage and loss modulus master curves were fitted accordingly, as shown in the following Figure 7.

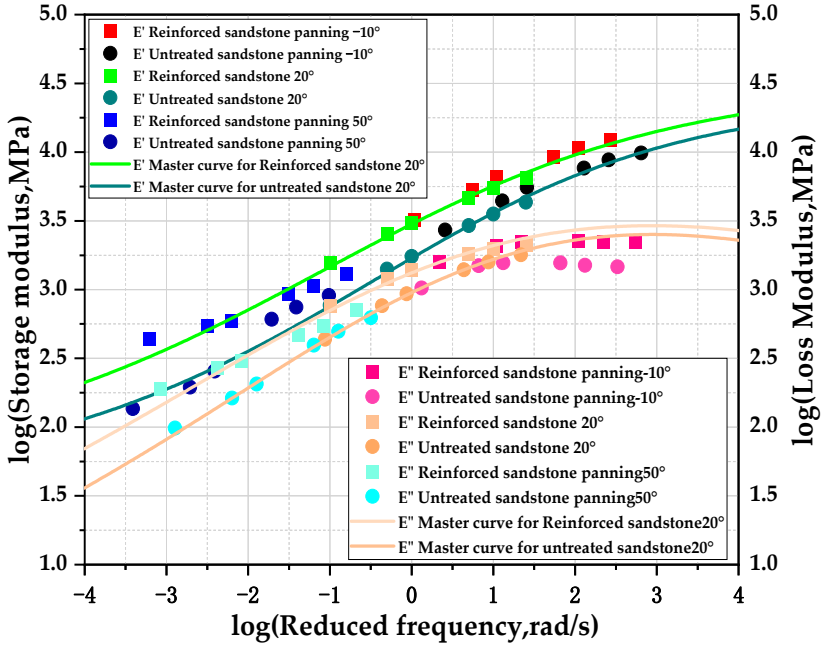


Figure 7. Storage modulus master curve and loss modulus master curve at 20 °C.

As illustrated in Figure 7, the storage modulus master curve exhibits an S-shaped profile similar to that of the dynamic modulus master curve. The loss modulus curve displays a bell-shaped profile, analogous to the phase angle [18]. The R^2 value for the reinforced sandstone is 0.98. It is noteworthy that when related to the phase angle, storage modulus, and loss modulus master curves—the R^2 value for the dynamic modulus fitted to the master curve is reduced. However, reading the parameters improves the accuracy. At any frequency, the storage modulus is greater than the loss modulus, indicating that the mix is predominantly elastic. The storage modulus is higher at high frequencies and low temperatures, suggesting that the mix can store more energy and exhibit greater elasticity. Conversely, at high temperatures and low frequencies, increased friction between the aggregates results in higher viscosity, which raises the loss modulus and lowers the storage modulus [20]. The storage modulus and loss modulus of reinforced sandstone are greater than those of untreated sandstone. However, the rate of increase in the storage modulus is higher than that of the loss modulus, leading to reinforced sandstone achieving greater elasticity and overall modulus values. This indicates that the formation of a dense reticulation on the aggregate surface after soaking in the sodium silicate solution improves the material's elasticity, achieving the desired effect.

5.2.4. Other Theoretical Measures of Linear Elasticity

Cole-Cole plots [23], which illustrate the trend in loss modulus versus storage modulus for asphalt mixtures, and Black plots [24], which depict the trend in dynamic modulus versus phase angle, do not require the application of the time-temperature equivalence principle. Consequently, they can eliminate the effect of temperature on these measurements.

From Figure 8, the above Cole-Cole plot shows that the curve is characterized by an initial increase, followed by a decrease, and then a plateau. Concurrently, the storage modulus exhibits a significant rise, with the surface storage modulus approaching the loss modulus at high temperatures, closely aligning with the y = x curve. This indicates an increase in viscosity at high temperatures, while at low temperatures, the curve diverges from the y = x curve, suggesting an increase in elasticity. The fundamental trend in the black plot is a monotonic decrease, indicating that the data at low and medium temperatures adhere to the principle of temperature superposition. Furthermore, the data points for the enhanced sandstones form a more continuous curve compared to the untreated sandstones, which is a more favorable outcome [24,25]. However, at high temperatures, the trend in the range of phase angle changes deviates from a single trend. It is postulated that this deviation may be due to a transition [22].

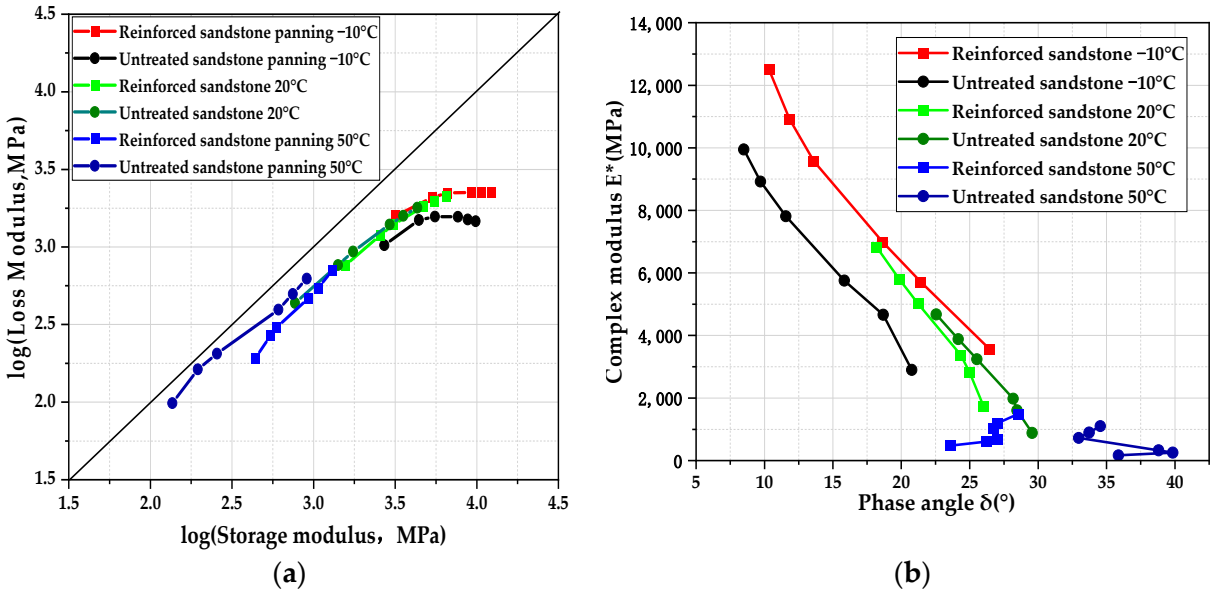


Figure 8. Cole-Cole plots and black plots. (**a**) Cole-Cole plots; (**b**) black plots.

5.2.5. Rutting Factor, Fatigue Factor, DSRFN Parameter

Dynamic modulus is one of the most important indicators for asphalt mixtures, as it can be used to describe the stiffness of asphalt mixtures. It can also be used to study the viscoelastic properties of a mixture, making it very important for the evaluation of asphalt mixtures. The dynamic modulus can also be used to calculate the rutting factor ($E^*/\sin\varphi$) [10,26], fatigue factor ($E^* \times \sin\varphi$) [27], and DSRFN parameter ($E'^2 \times \varepsilon/E''$, 15 °C and 0.005 rad/s) [28], and thus, it can express the high-temperature, fatigue, and low-temperature performance of a given mix, so a systematic study of the dynamic modulus is necessary to understand a mix. The results of the rutting and fatigue coefficients are shown in Figure 9 below. The values of dynamic modulus and phase angle at 15° are calculated from the shift factor (α_T) and the master curves of dynamic modulus and phase angle, and the results of DSRFN parameter calculation are shown in Table 6 below.

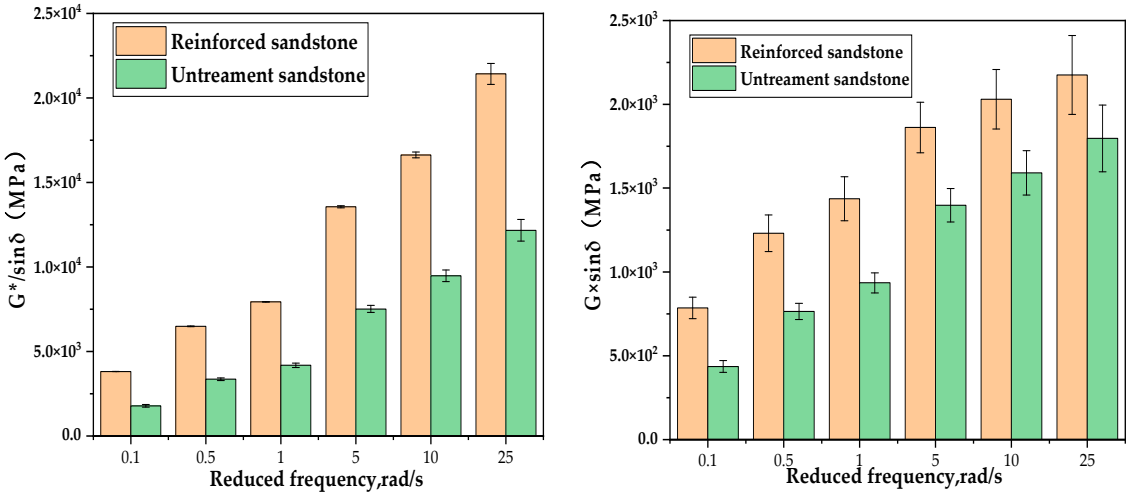


Figure 9. Rutting factor and fatigue factor. (**a**) Frequency Relation to Rutting Factor at 20°; (**b**) Frequency Relation to Fatigue Factor at 20°.

Table 6. DSRFn parameters.

Style	15°, 0.005 rad/s		DSRFn Parameters
	Dynamic Modulus/MPa	Phase Angle/°	
Reinforced sandstone	5623.41	19.95	11.58
Untreated sandstone	5248.07	25.12	8.065

Figure 9 illustrates that the rutting coefficient and fatigue coefficient of the mixtures exhibit an increase in frequency. A higher rutting coefficient indicates greater elasticity. The rutting coefficients of the reinforced sandstones demonstrate the greatest increase at 25 Hz. This suggests that an increase in velocity results in a reduction in permanent deformation. An increase in the fatigue coefficient indicates a reduction in the fatigue resistance of the mixture. As demonstrated in Table 6, the DSRFn coefficient shows an increase in this coefficient and a consequent reduction in low-temperature cracking resistance as the sandstone is reinforced. In conclusion, it is essential to consider and address crack resistance in conjunction with toughness reinforcement as the dynamic modulus increases.

6. Conclusions

In this study, the change in dynamic modulus of reinforced sandstone after immersion in sodium silicate solution was investigated by using the S-model and K-K relationship theory to fit the dynamic modulus master curve, assess the change in the behavior of the mix under various conditions, and predict the change in performance. Our specific conclusions are as follows:

1. Treating sandstone aggregates with sodium silicate can effectively improve the water absorption and mechanical properties of sandstone.
2. Treatment of sandstone aggregates with sodium silicate solution increases the dynamic modulus of asphalt mixtures by about 45%, reducing the phase angle and allowing the mix to exhibit greater elastic behavior, increasing the rutting factor, and significantly improving the high temperature stability of the mix.
3. The aforementioned sigmoidal function combined with the Kramers–Kronig relationship can be used to predict values of dynamic modulus, phase angle, storage modulus, and loss modulus over a wide frequency range, and the master curve can be used to investigate the linear viscoelastic behavior of the mix.

4. At high temperatures, the phase angle complicates the viscoelastic behavior, and the value of the phase angle does not vary with the smoothed master curve.
5. The dynamic modulus increases, the permanent deformation decreases, but the cracking resistance will be reduced. for high modulus, it is necessary to consider its toughening treatment.

Author Contributions: B.Z.: Writing—original draft; S.J.: Resources; N.Z.: Writing review & editing; J.L.: Investigation; Y.W.: Date curation. All authors have read and agreed to the published version of the manuscript.

Funding: This research did not receive any specific grant from funding agencies in the public, commercial, or not-for-profit sectors.

Data Availability Statement: Data available on request from the authors.

Conflicts of Interest: Author Shuangquan Jiang was employed by the company Sichuan Highway and Bridge Construction Group Limited. Author Jinduo Liu was employed by the company Jiaoke Transport Consultans Ltd. The remaining authors declare that the research was conducted in the absence of any commercial or financial relationships that could be construed as a potential conflict of interest.

References

1. Fan, J.; Xu, G.; Zhu, Y.; Cai, Z. Feasibility of Siliceous Sandstone Utilization in Porous Asphalt Mixture. *J. Transp. Eng. Part B Pavements* **2023**, *149*, 04022069. [CrossRef]
2. Li, H.; Guo, X.; Xin, J.; Li, Y.; Zhang, F.; Zhao, G.; Guo, P.; Sheng, Y. Study on the Characteristics of Sandstone and Feasibility to Replace Limestone in Cement Stabilized Macadam Base. *Int. J. Pavement Res. Technol.* **2023**, *16*, 1419–1438. [CrossRef]
3. Bao, X.; Yao, L. Study on road performance of sandstone for asphalt concrete surface. *Highway* **2014**, *59*, 243–246.
4. Ma, X. Application of sandstone SMA-13 mixture in asphalt surface layer. *Highw. Transp. Sci. Technol.* **2016**, *12*, 47–48.
5. Li, B.; Liu, J.; Bian, K.; Ai, F.; Hu, X.; Chen, M.; Liu, Z. Experimental study on the mechanical properties weakening mechanism of siltstone with different water content. *Arab. J. Geosci.* **2019**, *12*, 656. [CrossRef]
6. Chen, W.; Dai, P.; Yuan, P.; Zhang, J. Effect of inorganic silicate consolidation on the mechanical and durability performance of sandstone used in historical sites. *Constr. Build. Mater.* **2016**, *121*, 445–452. [CrossRef]
7. Yu, M.; Fang, J.; Zhao, L.; Song, K. Experimental study on unconfined compressive strength of water glass modified recycled aggregate. *Soil. Eng. Found.* **2023**, *37*, 315–317+334.
8. Tang, S.; Jiang, Z. Experimental study on impregnation effect of water glass on sandstone. *Chongqing Archit.* **2013**, *12*, 55–56.
9. *JTG E42-2005*; Test Methods of Aggregate for Highway Engineering. People's Transportation Press: Beijing, China, 2005. (In Chinese)
10. Jin, D.; Mohammadi, S.; Xin, K.; Yin, L.; You, Z. Laboratory performance and field demonstration of asphalt overlay with recycled rubber and tire fabric fiber. *Constr. Build. Mater.* **2024**, *438*, 136941. [CrossRef]
11. Jin, D.; Yin, L.; Nedrich, S.; Boateng, K.A.; You, Z. Resurface of rubber modified asphalt mixture with stress absorbing membrane interlayer: From laboratory to field application. *Constr. Build. Mater.* **2024**, *441*, 137452. [CrossRef]
12. Bonaquist, R.F. *Ruggedness Testing of the Dynamic Modulus and Flow Number Tests with the Simple Performance Tester*; The National Academies Press: Washington, DC, USA, 2008.
13. Nivedya, M.; Murru, P.T.; Veeraragavan, A.; Krishnan, J.M. Estimation of dynamic modulus of Bitumen Stabilized Mixes. *Constr. Build. Mater.* **2017**, *136*, 202–216. [CrossRef]
14. Li, H. Viscoelastic Mechanical Response Analysis of Asphalt Mixture and Asphalt Pavement under Dynamic and Static Loads. Ph.D. Thesis, Jilin University, Changchun, China, 2022.
15. Li, P.; Rao, W.; Feng, Z.; Li, J. Influence of test conditions and main curve of dynamic response of asphalt mixture. *J. Zhengzhou Univ. (Eng. Sci.)* **2016**, *37*, 1–5+11.
16. Luo, R.; Liu, H. Improving the Accuracy of Dynamic Modulus Master Curves of Asphalt Mixtures Constructed Using Uniaxial Compressive Creep Tests. *J. Mater. Civ. Eng.* **2017**, *29*, 04017032. [CrossRef]
17. Liu, H.; Luo, R. Development of master curve models complying with linear viscoelastic theory for complex moduli of asphalt mixtures with improved accuracy. *Constr. Build. Mater.* **2017**, *152*, 259–268. [CrossRef]
18. Ma, L.; Wang, H.; Ma, Y. Viscoelasticity of Asphalt Mixture Based on the Dynamic Modulus Test. *J. Mater. Civ. Eng.* **2024**, *36*, 3. [CrossRef]
19. Tschoegl, N.W. *The Phenomenological Theory of Linear Viscoelastic Behavior: An Introduction*; Springer: Berlin/Heidelberg, Germany, 2012.
20. Booij, H.C.; Thoone, G.P.J.M. Generalization of Kramers-Kronig transforms and some approximations of relations between viscoelastic quantities. *Rheol. Acta* **1982**, *21*, 15–24. [CrossRef]

21. Yang, X.; You, Z. New Predictive Equations for Dynamic Modulus and Phase Angle Using a Nonlinear Least-Squares Regression Model. *J. Mater. Civ. Eng.* **2015**, *27*, 3. [CrossRef]
22. Zaoutsos, S.; Papanicolaou, G.; Cardon, A. On the non-linear viscoelastic behaviour of polymer-matrix composites. *Compos. Sci. Technol.* **1998**, *58*, 883–889. [CrossRef]
23. Olard, F.; Di Benedetto, H. General "2S2P1D" model and relation between the linear viscoelastic behaviours of bituminous binders and mixes. *Road Mater. Pavement Des.* **2003**, *4*, 185–224.
24. Wu, W.; Jiang, W.; Xiao, J.; Yuan, D.; Wang, T.; Xing, C. Analysis of thermal susceptibility and rheological properties of asphalt binder modified with microwave activated crumb rubber. *J. Clean. Prod.* **2022**, *377*, 134488. [CrossRef]
25. Zhu, J.; Ahmed, A.; Said, S.; Dinegdae, Y.; Lu, X. Experimental analysis and predictive modelling of linear viscoelastic response of asphalt mixture under dy-namic shear loading. *Constr. Build. Mater.* **2022**, *328*, 127095. [CrossRef]
26. Xiao, X.; Wang, J.; Li, J.; Xiao, F. Dynamic characteristics and damage evolution behaviour of highly viscous and highly elastic asphalt concrete under freeze-thaw cycle. *China Highw. J.* **2023**, *36*, 64–76.
27. Ma, F.; An, Q.; Fu, Z.; Wen, Y.; Hou, Y.; Tang, Y. Effect of nano ZnO/TiO_2 on the performance of basalt fibre modified asphalt. *Funct. Mater.* **2023**, *54*, 8192–8198.
28. Chen, Z.; Zhang, H.; Duan, H. Investigation of ultraviolet radiation aging gradient in asphalt binder. *Constr. Build. Mater.* **2020**, *246*, 118501. [CrossRef]

Disclaimer/Publisher's Note: The statements, opinions and data contained in all publications are solely those of the individual author(s) and contributor(s) and not of MDPI and/or the editor(s). MDPI and/or the editor(s) disclaim responsibility for any injury to people or property resulting from any ideas, methods, instructions or products referred to in the content.